Importance of Aromatic Content for Peptide/Single-Walled Carbon Nanotube Interactions

ARTICLE *in* JOURNAL OF THE AMERICAN CHEMICAL SOCIETY · OCTOBER 2005

Impact Factor: 12.11 · DOI: 10.1021/ja050747v · Source: PubMed

J|A|C|S
ARTICLES
Published on Web 08/12/2005

Importance of Aromatic Content for Peptide/Single-Walled Carbon Nanotube Interactions

Vasiliki Zorbas,[†] Amy L. Smith,[†] Hui Xie,[†,‡] Alfonso Ortiz-Acevedo,[†] Alan B. Dalton,[‡,||] Gregg R. Dieckmann,[†,‡] Rockford K. Draper,[†,‡,§] Ray H. Baughman,[†,‡] and Inga H. Musselman*[,†,‡]

Contribution from Department of Chemistry, NanoTech Institute, and Department of Molecular and Cell Biology, The University of Texas at Dallas, 2601 North Floyd Road, Richardson, Texas 75080

Received February 4, 2005; E-mail: imusselm@utdallas.edu

Abstract: We have previously demonstrated that a designed amphiphilic peptide helix, denoted nano-1, coats and debundles single-walled carbon nanotubes (SWNTs) and promotes the assembly of these coated SWNTs into novel hierarchical structures via peptide−peptide interactions. The purpose of this study is to better understand how aromatic content impacts interactions between peptides and SWNTs. We have designed a series of peptides, based on the nano-1 sequence, in which the aromatic content is systematically varied. Atomic force microscopy measurements and optical absorption spectroscopy reveal that the ability to disperse individual SWNTs increases with increasing aromatic residues in the peptide. Altogether, the results indicate that π-stacking interactions play an important role in peptide dispersion of SWNTs.

Introduction

Applications ranging from high-strength, lightweight materials to nanoscale electronic devices have been investigated for single-walled carbon nanotubes (SWNTs) owing to their extraordinary electrical and mechanical properties.[1] Biological materials, such as peptides, have opened new possibilities for the dispersion, separation, functionalization, and manipulation of SWNTs.[2−6] Although peptide/SWNT dispersions extend the already vast list of prospective applications of SWNTs to biophysical and biomedical areas, further research is required to better understand the interaction of SWNTs and biological materials.

There are a few reports of the noncovalent interactions of water-soluble proteins and SWNT surfaces.[7−9] Chen et al. used a novel cross-linking agent to noncovalently link ferritin and streptavidin-gold conjugated proteins to SWNTs.[7] One end of this reagent contained pyrene, whose aromatic pyrenyl group interacts with the SWNT surface through aromatic π-stacking. Zheng et al. demonstrated that DNA bases interact with SWNTs through π-stacking and, consequently, assist in the dispersion and separation of SWNTs.[10] Various forms of porphyrins also effectively noncovalently solubilize SWNTs, presumably assisted by the planarity of the porphyrin ring.[11,12] Other studies using polymers with benzyl and pyrenyl moieties involve π-stacking interactions for the solubilization of SWNTs.[13,14]

The importance of protein π-stacking interactions also has been demonstrated through the recent development of fullerene-specific antibodies.[15−18] The proposed C_{60} binding site in the crystal structure of an anti-C_{60} monoclonal antibody would utilize π-stacking interactions between the fullerene and the aromatic side chains of the amino acids, Phe, Tyr, and Trp for binding.[18]

From these studies, the emerging concept of π-stacking protein/nanotube interactions was applied to our design of a peptide, denoted nano-1, that can form amphiphilic helical structure, coat, and solubilize SWNTs.[6] Amphiphilicity is

[†] Department of Chemistry.
[‡] NanoTech Institute.
[§] Department of Molecular and Cell Biology.
[||] Present address: Department of Physics, University of Surrey, Guildford GU2 7XH, UK.

(1) Baughman, R. H.; Zakhidov, A. A.; de Heer, W. A. *Science* **2002**, *297*, 787−792.
(2) Wang, S. et al. *Nat. Mater.* **2003**, *2*, 196−200.
(3) Zheng, M. et al. *Science* **2003**, *302*, 1545−1548.
(4) Chen, R. J.; Bangsaruntip, S.; Drouvalakis, K. A.; Kam, N. W. S.; Shim, M.; Li, Y.; Kim, W.; Utz, P. J.; Dai, H. *Proc. Natl. Acad. Sci. U.S.A.* **2003**, *100(9)*, 4984−4989.
(5) Balavoine, F.; Shultz, P.; Richard, C.; Mallouh, V.; Ebbeson, T. W.; Mioskowski, C. *Angew. Chem., Int. Ed.* **1999**, *38*, 1912−1915.
(6) Dieckmann, G. R.; Dalton, A. B.; Johnson, P. A.; Razal, J.; Chen, J.; Giordano, G. M.; Muñoz, E.; Musselman, I. H.; Baughman, R.; Draper, R. K. *J. Am. Chem. Soc.* **2003**, *125*, 1770−1777.
(7) Chen, R. J.; Zhang, Y.: Wang, D.; Dai, H. *J. Am. Chem. Soc.* **2001**, *123*, 3838−3839.
(8) Karajanagi, S. S.; Vertegel, A. A.; Kane, R. S.; Dordick, J. S. *Langmuir* **2004**, *20*, 11594−11599.
(9) Lin, Y.; Allard, L. F.; Sun, Y.-P. *J. Phys. Chem. B.* **2004**, *108*, 3760−3764.
(10) Zheng, M.; Jagota, A.; Semke, E. D.; Diner, B. A.; McLean, R. S.; Lustig, S. R.; Richardson, R. E.; Tassi, N. G. *Nat. Mater.* **2003**, *2*, 338−342.
(11) Chen, J.; Collier, P. C. *J. Phys. Chem. B.* **2005**, *109*, 7605−7609.
(12) Li, H.; Zhou, B.; Lin, Y.; Gu, L.; Wang, W.; Fernando, K. A. S.; Kumar, S.; Allard, L. F.; Sun, Y.-P. *J. Am. Chem. Soc.* **2004**, *126*, 1014−1015.
(13) Star, A. et al. *Angew. Chem., Int. Ed.* **2001**, *40*, 1721−1725.
(14) Carillo, A.; Swartz, J. A.; Gamba, J. M.; Kane, R. S. *Nano Lett.* **2003**, *3*(10), 1437−1440.
(15) Wise, K. E.; Park, C.; Siochi, E. J.; Harrison, J. S. *Chem. Phys. Lett.* **2004**, *391*, 207−211.
(16) Chen, B.-X.; Wilson, S. R.; Das, M.; Coughlin, D. J.; Erlanger, B. F. *Proc. Natl. Acad. Sci. U.S.A.* **1998**, *95(18)*, 10809−10813.
(17) Erlanger, B. F.; Chen, B.-X.; Zhu, M.; Brus, L. *Nano Lett.* **2003**, *1*(9), 465−467.
(18) Braden, B. C.; Goldbaum, F. A.; Chen, B.-X.; Kirschner, A. N.; Wilson, S. R.; Erlanger, B. F. *Proc. Natl. Acad. Sci. U.S.A.* **2000**, *97*(22), 12193−12197.

Table 1. Amphiphilic Helical Peptides Designed to Test the Roles of Aromatic Residues and Helical Structure on Peptide/SWNT Interactions

$(V_aL_d)_{4/4}$	E VEALEKK VAALESK VQALEKK VEALEHG
$(V_aF_d)_{4/4}$	E VEAFEKK VAAFESK VQAFEKK VEAFEHG
$(F_aF_d)_{4/4}$	E FEAFEKK FAAFESK FQAFEKK FEAFEHG
$(V_aF_d)_{1/4}$	E VEAFEKK Y

[a] Each seven residue repeat represents one helix heptad. Peptides $(V_aL_d)_{4/4}$, which is the previously well-characterized peptide CoilV_aL_d,[21] $(V_aF_d)_{4/4}$, and $(F_aF_d)_{4/4}$, have varying numbers of Phe (F) residues in the *a* and *d* positions (0, 4, and 8, respectively). The peptides $(V_aF_d)_{1/4}$ and $(V_aF_d)_{4/4}$ contain 1 and 4 heptads, respectively.

achieved through appropriate placement of apolar and polar residues in the peptide primary sequence such that residues *a* and *d* in the repeating heptad, denoted $(a,b,c,d,e,f,g)_n$, form a hydrophobic face and residues *b*, *c*, *e*, *f*, and *g* form a hydrophilic face. The *a* and *d* positions of each heptad in nano-1 are occupied by the hydrophobic residues valine (Val) and phenylalanine (Phe), respectively.[6] Phe, being aromatic, should interact effectively with the SWNT surface via π-stacking. We have previously demonstrated that nano-1 indeed isolates individual SWNTs[19] and enables hierarchical assembly of peptide-wrapped SWNTs into novel structures.[20]

The aim of this study is to better understand how the aromatic content in the peptide affects the dispersion of SWNTs. The importance of aromaticity in amphiphilic helical peptides was tested using a designed series of peptides that vary in the number of aromatic residues on the hydrophobic surface of the helix. The peptides $(V_aL_d)_{4/4}$, which is the previously well-characterized peptide CoilV_aL_d,[21] nano-1 (also called $(V_aF_d)_{4/4}$ in this manuscript), and $(F_aF_d)_{4/4}$, have varying numbers of Phe residues in the *a* and *d* positions (0, 4, and 8, respectively) (Table 1). The nomenclature $(X_aY_d)_{z/4}$ describes the peptides using one letter amino acid codes (X, Y) located at the *a* and *d* positions of the α-helix heptad as indicated by the alphabetical subscripts $(_a, _d)$. The fraction subscript $(_{z/4})$ conveys the peptide length in which the numerator indicates the number of heptads with that *a* and *d* sequence out of the four possible heptads in the peptide sequence. The degree of folding of a peptide designed to form a helical structure depends on sequence length. Therefore, we also investigated the role of aromatic content on SWNT dispersion in the absence of secondary structure effects by varying the length of the nano-1 sequence using $(V_aF_d)_{1/4}$, which contains only one heptad (Table 1). Optical absorption spectroscopy and atomic force microscopy (AFM) measurements revealed that the ability to disperse individual SWNTs increases with increasing aromatic amino acid content on the hydrophobic face of the amphiphilic helix.

Experimental Section

Peptide Synthesis and Purification. The synthesis and purification of all peptides were performed using previously described procedures.[6,19] The identities of the pure peptides were verified using electrospray ionization mass spectrometry (HT Laboratories).

Peptide/Nanotube Sample Preparations. A solution of 100 μM $(V_aL_d)_{4/4}$ was prepared using deionized water, and the peptide concentration was verified using quantitative amino acid analysis (analysis done by Biopolymer Lab at Brigham and Women's Hospital) and a Beer's Law standard calibration curve. Solutions of 100 μM $(F_aF_d)_{4/4}$ and $(V_aF_d)_{4/4}$ peptides, as well as 100 and 400 μM $(V_aF_d)_{1/4}$, were prepared using deionized water. Peptide concentrations were verified using ultraviolet molecular absorption spectrometry, with the peptide extinction coefficients calculated based on the extinction coefficients of the chromophores Phe and Tyr (197 L mol^{-1} cm^{-1} at 257 nm, 1420 L mol^{-1} cm^{-1} at 276 nm, respectively). The calculated extinction coefficients were also verified using Beer's Law standard calibration curves.

SWNTs produced by high-pressure decomposition of carbon monoxide (HiPco process)[22] were obtained from Carbon Nanotechnologies, Inc. Between 1.0 and 1.3 mg of HiPco SWNTs were weighed in Eppendorf tubes using a Mettler H251 analytical balance. To the tubes, a 1 mL volume of 100 or 400 μM peptide was added. The mixtures were vortexed for approximately 1 min and then sonicated using a VWR Scientific Branson Sonifier 250 with the sample immersed in an ice water bath. The 2 mm tip was placed into the samples approximately one-third of the distance from the surface. Samples were sonicated for 1 min at a power level of 10 W.

The sonicated samples were first centrifuged in an Eppendorf 5417C centrifuge for 10 min at 700 × *g*. The upper 75% of the supernatant was recovered using a small-bore pipet, avoiding sediment at the bottom, and transferred to a Beckman centrifuge tube for further centrifugation. Samples were then centrifuged for 30 min at 50 000 × *g* in a Beckman TL-100 ultracentrifuge with the temperature controlled at 4 °C. The upper 50% of the supernatant was recovered using a small-bore pipet, avoiding sediment at the bottom, and transferred to a clean tube. This centrifugation procedure was applied to all peptide/SWNT samples, except that centrifugation at a reduced speed (500 × *g* for 10 min) was necessary for 100 μM $(V_aF_d)_{1/4}$/SWNT samples. All peptide/SWNT preparations were performed three or more times to ensure reproducibility. The AFM height (diameter) statistics for the peptide/SWNT samples (Figures 3, 6) were taken from three independent sample preparations. Single factor analysis of variance (ANOVA), performed at the 95% confidence level, revealed that the three separate sample preparations conducted for each peptide/SWNT were statistically similar.

The supernatants were diluted 10-fold with deionized water, and 10 μL volumes were dropped onto freshly cleaved muscovite mica (Asheville-Schoonmaker Mica Co.). Samples were placed in a desiccator to dry for 24 h prior to imaging by AFM. Peptide control samples, lacking SWNTs, were also prepared using the identical sample preparation procedure. AFM images of the different peptide control samples exhibited no SWNT-like features, demonstrating that the peptides alone do not form fibrillar structures (Supporting Information).

Atomic Force Microscopy. AFM experiments were performed in air under ambient conditions using a Digital Instruments, Inc. Nanoscope III Multimode Scanning Probe Microscope operated in the TappingMode. The AFM "J" scanner was calibrated using a NanoDevices, Inc. standard consisting of lines with 2 μm pitch and 20 nm height, dimensions similar to those of SWNTs. The height calibration was verified using hydrofluoric acid etched pits in muscovite mica where 2 nm steps are observed along the long axis and 1 nm steps are observed along the short axis.[23] AFM images (2.0 × 2.0 μm^2) for height analysis of peptide-wrapped SWNTs were then acquired using a reduced Z-limit range (100−200 V) and cantilevers with force constants and average resonant frequencies of 5.0 N m^{-1} and 180 kHz, respectively.[19] Larger image sizes of 10 μm were necessary for length analysis of peptide-wrapped SWNTs.

(19) Zorbas, V.; Ortiz-Acevedo, A.; Dalton, A. B.; Yoshida, M. M.; Dieckmann, G. R.; Draper, R. K.; Baughman, R. H.; Yacaman, M. J.; Musselman, I. H. *J. Am. Chem. Soc.* **2004**, *126*, 7222−7226.
(20) Dalton, A. B. et al. *Adv. Funct. Mater.* **2004**, *14*, 1147−1151.
(21) Ogihara, N. L.; Weiss, M. S.; DeGrado, W. F.; Eisenberg, D. *Protein Sci.* **1999**, *8*, 1400−1409.
(22) Nikolaev, P.; Bronikowski, M.; Bradley, R.; Rohmund, F.; Colbert, D.; Smith, K.; Smalley, R. E. *Chem. Phys. Lett.* **1999**, *313*, 91−97.
(23) Nagahara, L. A.; Hashimoto, K.; Fujishima, A. *J. Vac. Sci. Technol., B.* **1994**, *12*(3), 1694−1697.

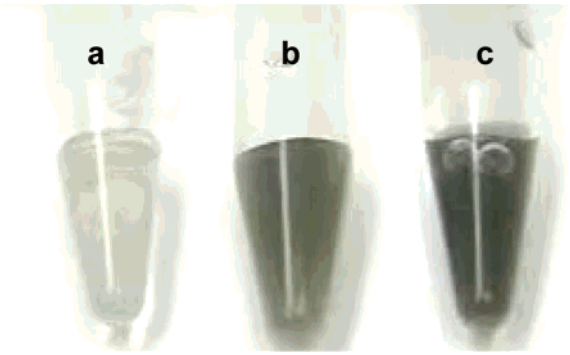

Figure 1. Photograph of Eppendorf tubes showing 50 000 × *g* supernatants of (a) $(V_aL_d)_{4/4}$/SWNT, (b) $(V_aF_d)_{4/4}$/SWNT, and (c) $(F_aF_d)_{4/4}$/SWNT samples. Differences among the peptide/SWNT dispersions were visually observed by a disparity of supernatant color intensity that qualitatively indicates the amount of dispersed SWNTs.

Ultraviolet−Visible−Near Infrared (UV−vis−NIR) Spectrophotometry. Peptide/SWNT dispersions were prepared following the described sample preparation procedures using D_2O in place of deionized water. Absorption spectra of peptide/SWNT dispersions in D_2O were obtained using a common D_2O blank in a Perkin-Elmer Lamda 900 UV−vis−NIR spectrophotometer.

Circular Dichroism (CD) Spectroscopy. CD spectra were acquired at 25 °C using an Aviv model 202 circular dichroism spectrometer and a 1 mm path length rectangular quartz cuvette. Spectra were collected from 190 to 260 nm at 1 nm intervals using a 6 s dwell-time at each wavelength increment.

Results

$(V_aL_d)_{4/4}$/SWNT, $(V_aF_d)_{4/4}$/SWNT, and $(F_aF_d)_{4/4}$/SWNT dispersions were generated using an identical sample preparation procedure in which a mixture of peptide solution (1 mL, 100 μM) and solid SWNTs (1.0−1.3 mg) were sonicated (1 min, 10 W) and centrifuged (50 000 × *g*, 30 min) yielding dispersions (supernatants), which were removed from the undispersed solid. Peptide/SWNT sample preparations were repeated at least three times for each peptide to ensure reproducibility. Differences among the peptide/SWNT dispersions were visually observed by a disparity of supernatant color intensity that qualitatively indicates the amount of dispersed SWNTs. Based solely on the supernatant color intensity of $(V_aL_d)_{4/4}$/SWNT (faint gray), $(V_aF_d)_{4/4}$/SWNT (gray), and $(F_aF_d)_{4/4}$/SWNT (dark gray), the amount of SWNTs that were solubilized appears to have increased with an increasing number of aromatic amino acids in the peptide sequence (Figure 1).

Another striking difference among the peptide/SWNT dispersions was discerned from AFM images. HiPco SWNTs are typically less than 1 μm in length and range from 0.7 to 1.5 nm in diameter.[22] Unusually long SWNTs, with several longer than the image size (>10.0 μm), were observed in the AFM images of $(V_aF_d)_{4/4}$/SWNT and $(F_aF_d)_{4/4}$/SWNT dispersions (Figure 2b and c). In contrast, $(V_aL_d)_{4/4}$/SWNT supernatants exhibited shorter SWNTs ranging from 0.1 to 6.7 μm with an average length of 0.7 ± 0.6 μm (four 10.0 × 10.0 μm^2 images; n = 200) (Figure 2a).

AFM height measurements, which provide an accurate measure of SWNT diameter, revealed another difference among the various peptide/SWNT dispersions (Figures 2 and 3). AFM height analysis of $(F_aF_d)_{4/4}$/SWNT dispersions provided a diameter distribution ranging from 0.8 to 6.5 nm, with an average diameter of 2.1 ± 1.1 nm (four 2.0 × 2.0 μm^2 images, n = 205). The diameters of the nanotubes in the $(V_aF_d)_{4/4}$/SWNT dispersion ranged from 0.9 to 6.9 nm, with an average diameter of 2.4 ± 1.3 nm (four 2.0 × 2.0 μm^2 images, n = 215). Considering the reported diameters of pristine SWNTs[22] and that the peptide coating can add an additional 1 to 3 nm, these height measurements for $(F_aF_d)_{4/4}$/SWNT and $(V_aF_d)_{4/4}$/SWNT dispersions suggest that the majority of the observed nanotubes are individual SWNTs wrapped with peptide. In contrast, the diameter of features in $(V_aL_d)_{4/4}$/SWNT dispersions ranged from 1.0 to 12.6 nm with an average diameter of 4.4 ± 2.3 nm (six 2.0 × 2.0 μm^2 images, n = 200), suggesting that very few of the features correspond to individual SWNTs, but rather they appear as small bundles of SWNTs. T-tests for nonhomogeneous variances, performed at the 95% confidence level for both $(V_aL_d)_{4/4}$ versus $(F_aF_d)_{4/4}$ and $(V_aL_d)_{4/4}$ versus $(V_aF_d)_{4/4}$, revealed that the average SWNT diameters can be distinguished.

Figure 4 presents UV−vis−NIR absorption spectra of the peptide/SWNT dispersions. The confinement to the graphene electronic states around the SWNT circumference causes the 1D SWNT electronic band structure to have a series of sharp von Hove singularities.[24] The optical absorption spectra of individual SWNTs are characterized by a series of relatively sharp transitions at energies related to these von Hove singularities. Aggregation of SWNTs into bundles substantially broadens the interband transitions in the absorption spectra. This broadening is attributed to intertube van der Waals interactions that disturb the electronic structure of SWNTs.[25] The broadened and red-shifted absorption spectrum of the $(V_aL_d)_{4/4}$/SWNT sample (Figure 4a) demonstrates that the SWNTs in this sample are predominately bundled. Optical absorption spectroscopy and AFM of $(V_aL_d)_{4/4}$/SWNT dispersions revealed that the absence of aromatic amino acids on the apolar surface of the amphiphilic helix, in this case, results in a suspension of predominately bundled SWNTs.

The absorption spectra of the $(V_aF_d)_{4/4}$/SWNT (Figure 4b) and $(F_aF_d)_{4/4}$/SWNT (Figure 4c) samples show more pronounced features compared to the $(V_aL_d)_{4/4}$/SWNT sample. These well-resolved spectral features corroborate the AFM evidence of SWNT debundling in aqueous solution by $(V_aF_d)_{4/4}$ and $(F_aF_d)_{4/4}$. The absorption peaks of these two spectra match exactly in wavelength but differ in intensity. The matching absorption spectral traces (Figure 4) and the similar diameter distributions (Figure 3) of the $(V_aF_d)_{4/4}$/SWNT and $(F_aF_d)_{4/4}$/SWNT samples indicate that both peptides are capable of dispersing individual SWNTs. The increased intensity of the absorption spectrum for the $(F_aF_d)_{4/4}$/SWNT dispersion, compared to that of the $(V_aF_d)_{4/4}$/SWNT dispersion, suggests that additional Phe residues increase the amount of SWNTs that are dispersed. From these data, it can be concluded that the isolation of individual SWNTs is achieved with an amphiphilic peptide design containing four aromatic amino acids ($(V_aF_d)_{4/4}$), although the addition of more aromatic amino acids in the *a* and *d* positions ($(F_aF_d)_{4/4}$) results in an increased amount of SWNTs that are dispersed. This effect can be explained in terms of both the sequence and the structure of the two peptides. Sequences that place more aromatic amino acids in the *a* and *d* positions to interact with the SWNT surface

(24) Dresselhaus, M. S., Dresselhaus G., Eds. *Carbon Nanotubes: Synthesis, Structure, Properties and Applications*; Springer: New York, 2001; Vol. 81, pp 341−347.
(25) O'Connell, M. J. et al. *Science* **2002**, *297*, 593−596.

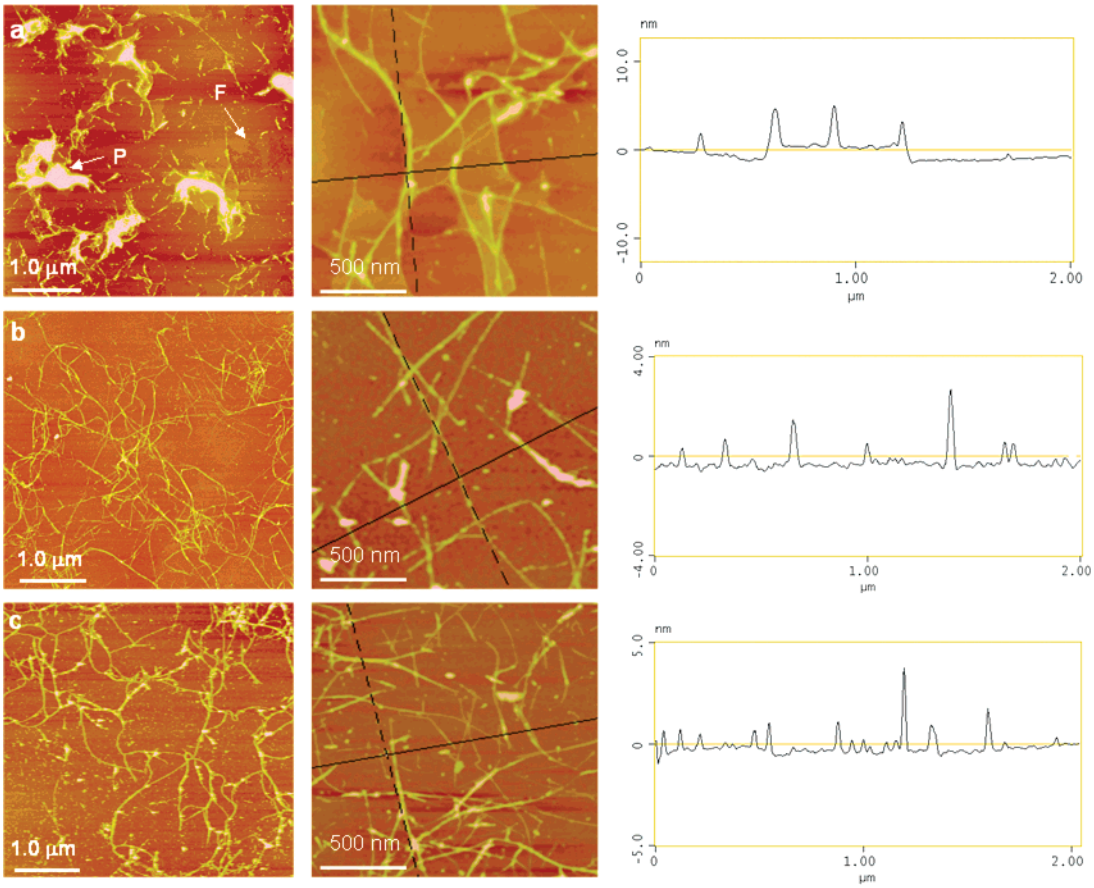

Figure 2. AFM images (a) $(V_aL_d)_{4/4}$/SWNT, (b) $(V_aF_d)_{4/4}$/SWNT and (c) $(F_aF_d)_{4/4}$/SWNT samples. For each row: left, 10.0 × 10.0 μm^2 image; center, 2.0 × 2.0 μm^2 image; right, cross-sectional topological profile taken along the solid black line drawn in the corresponding center image. In the left panel of (a), arrow F points to peptide film and arrow P points to pools of peptide.

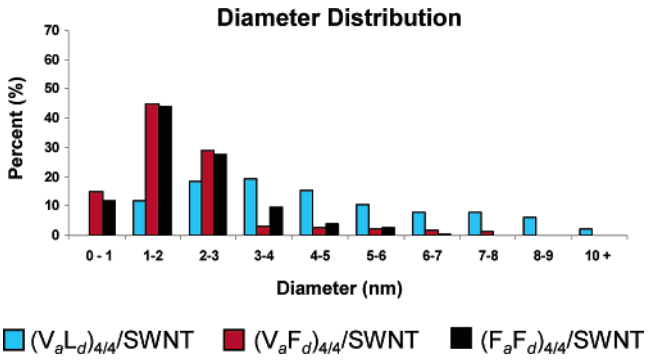

Figure 3. Diameter distributions (determined from AFM height measurements) of $(V_aL_d)_{4/4}$, $(V_aF_d)_{4/4}$, and $(F_aF_d)_{4/4}$ 50 000 × *g* dispersions of SWNTs. The diameters of $(V_aF_d)_{4/4}$/SWNT and $(F_aF_d)_{4/4}$/SWNT samples are indicative of debundled individual peptide-wrapped SWNTs, while the diameters of $(V_aL_d)_{4/4}$/SWNT samples appear to represent small SWNT bundles.

allow for increased π-stacking interactions, thereby enhancing SWNT dispersion. Moreover, CD data indicate that $(V_aF_d)_{4/4}$ is significantly less helical than $(F_aF_d)_{4/4}$ under similar conditions of peptide concentration and pH.[26] We expect that a more folded (helical) structure displays a hydrophobic surface more effectively and, therefore, better disperses SWNTs.

The inferior dispersing capability of $(V_aL_d)_{4/4}$ compared to that of $(V_aF_d)_{4/4}$ and $(F_aF_d)_{4/4}$ can be best explained by considering two controlling factors. First, without aromatic amino acids, $(V_aL_d)_{4/4}$ has a weaker interaction with the nanotube surface. As has been recently demonstrated with sodium dodecylbenzene sulfonate, compared to the widely used surfactant system of sodium dodecyl sulfate, π-stacking interactions increase the binding to SWNTs and hence increase the fraction of single tubes in solution.[27] Similarly, the stacking of aromatic amino acids onto the graphene SWNT surface allows for the dispersion of individual SWNTs. Second, the incorporation of aromatic groups into the helix apolar face decreases the ability of the peptides to self-associate.[26] This peptide self-association is revealed in AFM images and corresponding cross-sectional profiles of the $(V_aL_d)_{4/4}$/SWNT samples as a peptide film and as pools of peptide (Figure 2a). Conversely, free peptide is present only as small beads in the AFM images and corresponding cross-sectional profiles of the $(V_aF_d)_{4/4}$/SWNT and $(F_aF_d)_{4/4}$/SWNT dispersions. Peptides that self-associate to a greater degree (larger K_{Assoc}) should be less effective at dispersing SWNTs.

To examine the role of aromatic content on SWNT dispersion in the absence of secondary structure effects, the length of the four heptad $(V_aF_d)_{4/4}$ sequence was decreased to a one heptad $(V_aF_d)_{1/4}$ sequence (Table 1). Decreasing the sequence length of a peptide designed to form helical structures will impact the degree of folding. CD was utilized to characterize the peptide's ability to fold in aqueous solution, both alone and in the presence

(26) Acevedo-Ortiz, A. Ph.D. Thesis, University of Texas at Dallas, Richardson, TX, unpublished.

(27) Islam, M. F.; Rojas, E.; Bergey, D. M.; Johnson, A. T.; Yodh, A. G. *Nano Lett.* **2002** *3*(2), 269−273.

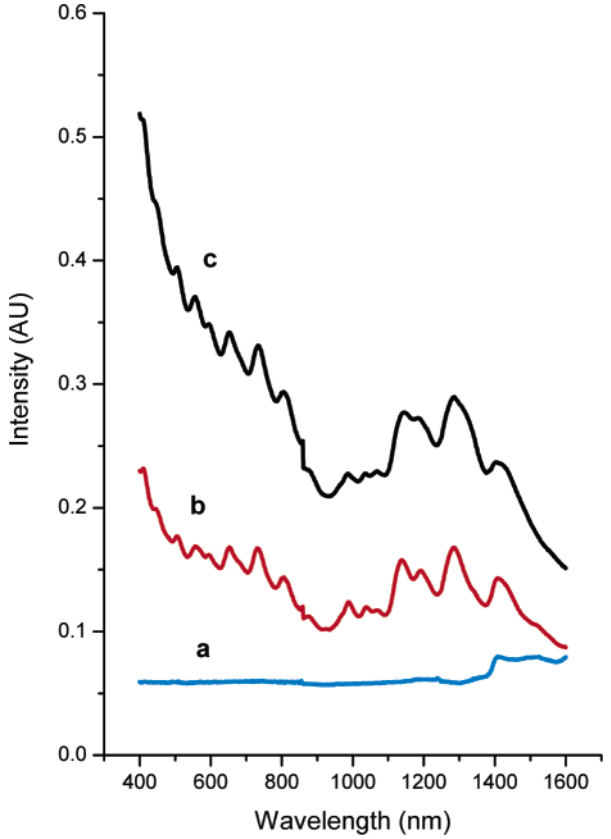

Figure 4. Absorption spectra of (a) $(V_aL_d)_{4/4}$/SWNT, (b) $(V_aF_d)_{4/4}$/SWNT, and (c) $(F_aF_d)_{4/4}$/SWNT samples. The sharp feature at ~860 nm is due to a grating and detector change associated with the spectrophotometer.

of SWNTs (Supporting Information). There were no predominant CD peaks indicative of α-helical secondary structure (negative features at 222 and 208 nm) for 100 and 400 μM $(V_aF_d)_{1/4}$, both in the presence and in the absence of SWNTs. This result reveals that the shorter peptide indeed does not adopt a significant degree of α-helical structure in aqueous solution as a function of increasing peptide concentration or as a result of stabilization by hydrophobic interactions between the peptide *a*/*d* face and the SWNT surface. As expected, this behavior is contrary to that reported for $(V_aF_d)_{4/4}$ (i.e., nano-1).[6] Therefore, the 100 and 400 μM $(V_aF_d)_{1/4}$ samples will allow us to examine the role of increasing aromatic content on dispersing SWNTs in the absence of amphiphilic helical structure.

The 100 μM $(V_aF_d)_{1/4}$/SWNT sample yielded a colorless 50 000 × *g* supernatant (not shown) suggesting minimal SWNT dispersion. AFM images (not shown) of this sample confirmed the absence of SWNTs. A lower centrifugation speed of 500 × *g* yielded a light gray supernatant. AFM images of this supernatant exhibited SWNTs ranging from 0.1 to 2.0 μm in length, with an average length of 0.3 ± 0.2 μm (three 10 × 10 μm^2 images; $n = 220$) (Figure 5a). AFM height measurements of the 500 × *g* $(V_aF_d)_{1/4}$/SWNT supernatant revealed a predominance of small SWNT bundles with diameters ranging from 0.8 to 18.2 nm, with an average diameter of 4.7 ± 2.6 nm (two 2 × 2 μm^2 images, $n = 64$) (Figure 6).

In contrast, when using the identical sonication and high-speed centrifugation procedure as with 100 μM $(V_aF_d)_{4/4}$, the 50 000 × *g* supernatant of 400 μM $(V_aF_d)_{1/4}$/SWNT was a homogeneous dark gray color. The AFM image of the 50 000 × *g* supernatant of 400 μM $(V_aF_d)_{1/4}$/SWNT samples (Figure

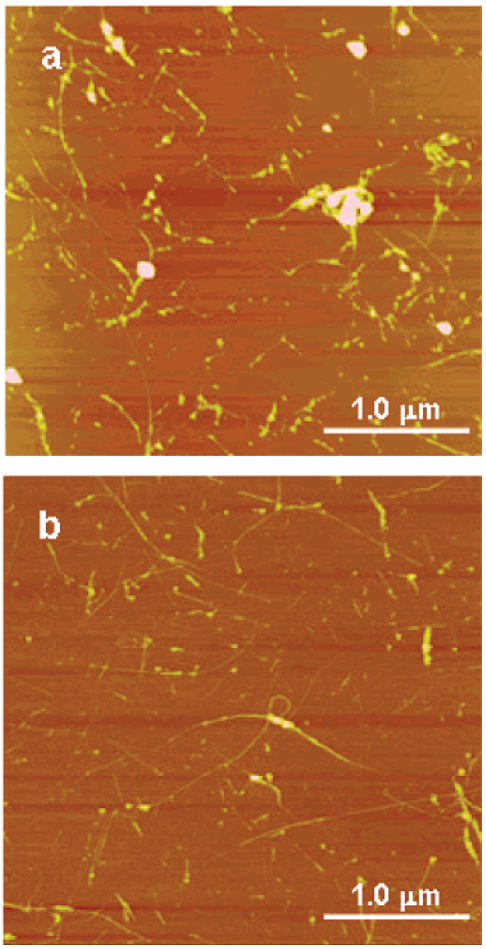

Figure 5. AFM images (5.0 × 5.0 μm^2) of (a) 500 × *g* supernatant of 100 μM $(V_aF_d)_{1/4}$/SWNT sample exhibiting predominately SWNT bundles and (b) 50 000 × *g* supernatant of 400 μM $(V_aF_d)_{1/4}$/SWNT sample showing individual SWNTs.

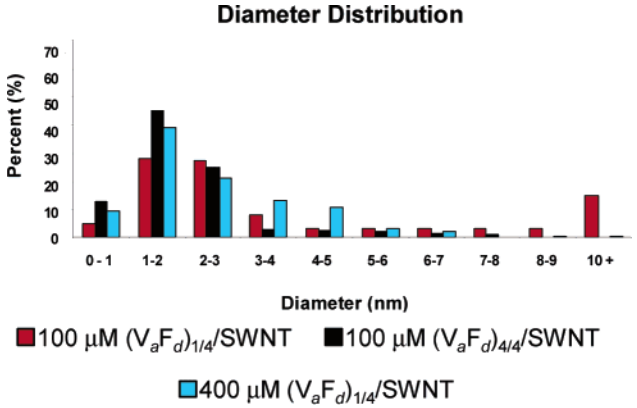

Figure 6. Diameter distributions (determined from AFM height measurements) of 500 × *g* supernatant of 100 μM $(V_aF_d)_{1/4}$ and 50 000 × *g* supernatant of 400 μM $(V_aF_d)_{1/4}$ and 100 μM $(V_aF_d)_{4/4}$ dispersions of SWNTs. Diameter distribution of the tubes in the 400 μM $(V_aF_d)_{1/4}$/SWNT sample is comparable to that of tubes in the 100 μM $(V_aF_d)_{4/4}$/SWNT sample in which both are indicative of debundled individual peptide-wrapped SWNTs. In contrast, diameters of tubes in the 100 μM $(V_aF_d)_{1/4}$/SWNT sample appear to represent SWNT bundles.

5b) exhibited SWNT-like features ranging in length from 0.1 to 4.2 μm, with an average length of 0.9 ± 0.6 μm (three 5.0 × 5.0 μm^2 images, $n = 205$). The diameters for the tubes in the 400 μM $(V_aF_d)_{1/4}$/SWNT dispersion ranged from 0.8 to 10.8 nm, with an average diameter of 2.6 ± 1.6 nm (four 2.0 × 2.0

μm^2 images, $n = 163$) suggesting the presence of predominately individual, peptide-wrapped SWNTs (Figure 6).

A t-test for nonhomogeneous variances, performed at the 95% confidence level, for 100 μM $(V_aF_d)_{4/4}$ versus 100 μM $(V_aF_d)_{1/4}$ revealed that the average SWNT diameters could be distinguished; however, a t-test for nonhomogeneous variances, performed at the 95% confidence level, for 100 μM $(V_aF_d)_{4/4}$ versus 400 μM $(V_aF_d)_{1/4}$ showed that the average SWNT diameters were statistically similar. Hence, the 400 μM $(V_aF_d)_{1/4}$ sample, which has the same number of aromatic residues in solution as 100 μM $(V_aF_d)_{4/4}$ but lacks helical structure, is still capable of dispersing SWNTs. The inability of the 100 μM $(V_aF_d)_{1/4}$ to do the same implies that π-stacking interactions are important in SWNT dispersion and demonstrates the importance of aromatic content for peptide−SWNT interactions. Interestingly, a t-test for nonhomogeneous variances, performed at the 95% confidence level, for 100 μM $(V_aF_d)_{4/4}$ versus 400 μM $(V_aF_d)_{1/4}$ revealed a statistical difference in average SWNT length, with the 100 μM $(V_aF_d)_{4/4}$/SWNT dispersions exhibiting longer SWNTs. There are two viable explanations for this result. First, the longer helical peptide may better bridge adjacent SWNTs, which is consistent with the designed structure of folded $(V_aF_d)_{4/4}$ (nano-1) intended to promote self-assembly through peptide−peptide interactions.[6,19] Second, the longer helical peptide may better coat the SWNTs and thereby protect them from possible breakage during sonication.[19]

Conclusions

The importance of aromatic residues was examined using a series of peptides that varied the number of phenylalanine residues on the hydrophobic surface of the helical peptide. Optical spectroscopy and AFM measurements revealed that sequences which placed more aromatic amino acids in the *a* and *d* positions were more effective at dispersing individual SWNTs. Isolation of individual SWNTs was achieved with an amphiphilic peptide design containing four aromatic amino acids in the *d* position ($(V_aF_d)_{4/4}$), although the addition of more aromatic amino acids in the *a* position ($(F_aF_d)_{4/4}$) resulted in an increased amount of SWNTs that were dispersed. Without aromatic amino acids in the apolar face of the amphiphilic helix ($(V_aL_d)_{4/4}$), only small bundles of SWNTs can be suspended, as this polypeptide self-associates and also lacks the ability to interact with the SWNT surface through π-stacking. The impact of aromatic content in the absence of secondary structure effects was further studied by varying the concentration of a one heptad sequence, $(V_aF_d)_{1/4}$, which does not fold into an α-helical conformation. CD spectra, correlated with AFM analyses, provided evidence of increased SWNT dispersion with increasing aromatic residues in solution. Altogether, these data demonstrate that π-stacking interactions between aromatic residues of a peptide and the graphene surface of a SWNT play an important role in peptide dispersion of SWNTs.

Acknowledgment. The support of this research by the Robert A. Welch Foundation [AT-1326 (I.H.M.)], the Department of Homeland Security (V.Z.), and the MIRROR Federal Initiative (A.O.-A.) are gratefully acknowledged.

Supporting Information Available: AFM images of peptide control samples and CD spectra of the 100 and 400 μM $(V_aF_d)_{1/4}$ samples, with and without SWNTs, are provided (PDF). This material is available free of charge via the Internet at http://pubs.acs.org.

JA050747V